NeuroImage xxx (2009) xxx–xxx

Contents lists available at ScienceDirect

NeuroImage

journal homepage: www.elsevier.com/locate/ynimg

Technical Note

A probabilistic MR atlas of the human cerebellum

Jörn Diedrichsen [a,*], Joshua H. Balsters [b], Jonathan Flavell [a], Emma Cussans [b], Narender Ramnani [b]

[a] Wolfson Centre for Cognitive and Clinical Neuroscience, School of Psychology, Adeilad Brigantia, University of Wales Bangor, Gwynedd LL572AS, UK
[b] Department of Psychology, Royal Holloway University of London, UK

ARTICLE INFO

Article history:
Received 7 May 2008
Revised 17 January 2009
Accepted 22 January 2009
Available online xxxx

ABSTRACT

The functional organization of the cerebellum is reflected in large part by the unique afferent and efferent connectivity of the individual cerebellar lobules. This functional diversity on a relatively small spatial scale makes accurate localization methods for human functional imaging and anatomical patient-based research indispensable. Here we present a probabilistic atlas of the cerebellar lobules in the anatomical space defined by the MNI152 template. We separately masked the lobules on T1-weighted MRI scans (1 mm isotropic resolution) of 20 healthy young participants (10 male, 10 female, average age 23.7 yrs). These cerebella were then aligned to the standard or non-linear version of the whole-brain MNI152 template using a number of commonly used normalization algorithms, or to a previously published cerebellum-only template (Diedrichsen, J., 2006. A spatially unbiased atlas template of the human cerebellum. NeuroImage 33, 127–138.). The resulting average overlap was higher for the cerebellum-only template than for any of the whole-brain normalization methods. The probabilistic maps allow for the valid assignment of functional activations to specific cerebellar lobules, while providing a quantitative measure of the uncertainty of such assignments. Furthermore, maximum probability maps derived from these atlases can be used to define regions of interest (ROIs) in functional neuroimaging and neuroanatomical research. The atlas, made freely available online, is compatible with a number of widely used analysis packages.

Introduction

The nature of cerebellar information processing is one of the most intriguing problems in systems neuroscience. While the local circuitry is relatively homogenous across the cerebellar cortex, the input–output relationships of different parts of the cerebellum are diverse, and are key to understand its functional organization. The existence of several independent cortico-cerebellar loops has been posited (Desmond et al., 1997; Middleton and Strick, 1997; Ramnani, 2006). In particular, lobules V, VI, VIIb and VIIIa have reciprocal connections with primary motor cortex, whereas Crus II has connections with area 46 in prefrontal cortex (Kelly and Strick, 2003). Thus, a number of functionally diverse lobules collectively occupy a spatially small volume. This makes the accurate localization of functional and anatomical data to specific cerebellar lobules very important.

A detailed understanding of structure–function relationships in the cerebellum requires therefore a reliable standard anatomical reference for the human cerebellum. One important step was the landmark publication of a cerebellar MR atlas by Schmahmann et al. (2000). In this atlas, a T1-weighted image of a single human cerebellum was coregistered to the MNI (Montreal Neurological Institute) template (Evans et al., 1993) and carefully annotated, providing researchers with a clear consensus about terminology. The atlas is now widely used, for example to annotate results from fMRI group analysis with lobular labels.

This latter use of the atlas, however, carries the risk of systematic mis-assignments of anatomical labels to locations. The problem arises because of the relatively high spatial variability of individual cerebellar structures after alignment to the MNI template space. For example, after affine whole-brain alignment the primary fissures and the intrabiventer fissures of different individuals spread over an area of more than 1.5 cm in the common atlas space (Diedrichsen, 2006), an area as wide as the neighboring lobules themselves. Therefore, we cannot expect that the spatial arrangement of structures in an individual cerebellum is representative of the spatial arrangement in a population of participants.

For neocortical cytoarchitecture, the problem has been addressed through the development of a set of probabilistic atlases (Amunts and Zilles, 2001; Toga et al., 2006). Using post-mortem histological and chemical measures, different cytoarchitectonic areas were identified in individual brains and aligned into MNI reference space. Data from these individuals was combined, and the resulting maps indicate the proportion of subjects in whom a specific cytoarchitectonic field occupies a location in MNI reference space. This provides a measure of the likelihood that a particular coordinate in MNI space is occupied by cortex with certain cytoarchitectonic properties, and can be used to assign anatomical labels to functional activation in an informed, systematic and unbiased fashion (Eickhoff et al., 2007). The approach can also be used to define regions of interest to test a-priori hypotheses (Eickhoff et al., 2006).

* Corresponding author. Fax: +44 01248 383768.
E-mail address: j.diedrichsen@bangor.ac.uk (J. Diedrichsen).
URL: http://www.bangor.ac.uk/pss412 (J. Diedrichsen).

1053-8119/$ – see front matter © 2009 Published by Elsevier Inc.
doi:10.1016/j.neuroimage.2009.01.045

Given the usefulness of probabilistic approaches to the anatomy of the neocortex, we thought to develop a similar tool for the human cerebellum. However, in the cerebellum a cyto-architectonic approach is not possible, as the local circuitry is homogenous, and we currently do not have reliable techniques to map the connectivity of the human cerebellum. Therefore, macro-anatomy currently provides the best source of information for classifying functionally distinct regions of the cerebellar cortex. In favor of a macro-anatomical approach is also that the subdivision of the cerebellar cortex into 10 lobules is relative invariant across normal healthy individuals and even across a range of mammalian species. Despite this invariance, there is inter-subject spatial variability in the ways that individual lobules occupy MNI reference space after registration. Here, we create a probabilistic representation of each of the cerebellar lobules and quantify this spatial variability.

In the development of probabilistic atlases, the choice of method used for registration or normalization of individual anatomies to the reference template is important. The spatial resolution of the normalization algorithm, the choice of reference template, and the involved preprocessing of the anatomical data will all influence the spatial variances of structures in reference space. Different normalization methods can potentially also lead to differences in the average location of structures in reference space, even if the same reference template is used. It is therefore important that the normalization method used to analyze the data matches as closely as possible the normalization method that is used to generate the atlas. To improve cerebellar alignment, we have recently developed a high-resolution template of the cerebellum and brainstem (SUIT, Diedrichsen, 2006) that considerably improves overlap compared to current whole-brain normalization methods. While the probabilistic atlas allows for the highest confidence of lobular assignments when using SUIT normalization, we also generated the atlas using a range of commonly used whole-brain normalization methods.

Methods

Participants

The structural images of twenty neurologically normal, healthy right-handed participants were used. There were ten male and ten female subjects, with ages ranging from 19 to 27, average 23.7 yrs. The racial composition of the sample reflects the diversity typical for fMRI studies with volunteers drawn from a University population: The sample included participants with Caucasian (14), East Asian (3), Indian (2), and African (1) racial origin. Structural images were acquired as part of two different studies, one approved by the Royal Holloway University of London Psychology Department Ethics Committee, one approved by the Ethics committee of Johns Hopkins Medical School. All participants gave written informed consent for their data to be reused.

Image acquisition

Ten participants were scanned using the 3 T Siemens Trio MRI scanner based at Royal Holloway University of London, UK. The other ten images were acquired on a 3 T Philips Intera system at Johns Hopkins Medical School, Maryland, US. All images were acquired using a T1 MPRAGE sequence with a voxel size of 1 mm^3, lasting approximately 5 min. All 20 participants are different from those used for the generation of the SUIT atlas (Diedrichsen, 2006).

Anatomy and parcellation

As a first step, we used an automatic algorithm (published as a SPM toolbox, Diedrichsen, 2006) to isolate the cerebellum from the surrounding tissue. This algorithm is based on a segmentation of voxels according to tissue types (white matter, gray matter, csf) using a probabilistic segmentation method (SPM5, Ashburner and Friston, 2005). Subsequently, cerebellar gray and white matter is separated from the cerebral gray and white matter using Bayesian inference.

On the individual anatomical scans we identified the cerebellar fissures (intraculminate, primary, superior posterior, horizontal, ansoparamedian, prebiventer, intrabiventer, secondary and posterolateral), using the labeled anatomical reference brain (Schmahmann et al., 2000). We started on the mid-saggital slice on which many anatomical landmarks are easily distinguishable, and then followed the fissures laterally. Based on these fissures, we created mask images for each lobule, with a value of one assigned to voxels that occupied lobular territory, while all other voxels were assigned a value of zero. Masking was conducted in FSLview (www.fmrib.ox.ac.uk/fsl) by drawing over anatomical T1 scans of the cerebellum. We grouped lobules I–IV into a single mask, and created separate masks for lobules V, VI, Crus I, Crus II, VIIb, VIIIa, VIIIb, IX, and X. The masks were then separated into the vermal, left, and right hemispheric part. The vermis was only defined for lobules VI–X, because in the anterior lobe the vermis does not have a clear anatomical boundary that separates it from the hemispheres (Schmahmann et al., 2000). The left and right hemispheres of the anterior lobe were divided along the midline. The resulting masks defined 28 compartments of the cerebellum. Coronal and horizontal views were used to validate and refine the assignment of individual voxels to lobules. Generation of the masks was refined until a consensus between the authors was reached.

Note that in the article we use the term lobule X to refer to both hemispheric and vermal part. Accordingly, we also use the term Crus I, to refer to Crus I proper plus its corresponding vermal component VIIaf, and the term Crus II to refer to Crus II plus its vermal component VIIat.

Normalization

To bring the lobular maps into a common reference space, we used six different normalization methods. These algorithms differed on three important factors: First, the spatial transformations allowed for different degrees of flexibility, varying from 12-parameter affine transformations to high-dimensional nonlinear transformations with a spatial resolution of up to 1 cm. Secondly, different methods employed varying degrees of tissue segmentation before or during normalization, including skull stripping (FLIRT), segmentation of white and gray matter (SPM segmentation), or cerebellar isolation (SUIT). Tissue segmentation reduces the influence of extra-cerebellar structures onto the normalization. Finally, different reference templates can be used. The most commonly used template, the standard MNI152, was generated by averaging 152 anatomical scans after correcting for overall brain size and orientation (Evans et al., 1993). This template provides very little anatomical detail on the cerebellum. To amend this situation, we have developed a high-resolution atlas template of the cerebellum by normalizing individual cerebella non-linearly to each other, before averaging them (Diedrichsen, 2006), resulting in a template with much better anatomical detail. Recently, the same technique has been applied to the whole brain, resulting in a new, non-linear version of the MNI152 template.

The following techniques were used:

(1) Affine: 12-parameter affine registration to the standard MNI152 template, without skull stripping using SPM5.
(2) FLIRT: 12-parameter affine registration to the nonlinear version of the MNI152 template, 2 mm, brain-only template using FLIRT (Jenkinson et al., 2002), which is part of the FSL-package (Smith et al., 2004). Anatomical images were skull-stripped before normalization.
(3) SPM2/5: Non-linear normalization without segmentation to the standard MNI152 template using cosine basis functions, after initial affine registration (Ashburner and Friston, 1999). This is the

Please cite this article as: Diedrichsen, J., et al., A probabilistic MR atlas of the human cerebellum, NeuroImage (2009), doi:10.1016/j.neuroimage.2009.01.045

standard algorithm for the "normalization" command in SPM 2/SPM5 (Friston et al., 1999). We used the default parameters (smoothing of source 8 mm FWHM, 25 mm cutoff, regularization = 1, within-brain weighting image for template).

(4) SPM segmentation: Simultaneous segmentation and normalization to the standard MNI152 template (Ashburner and Friston, 2005) as introduced in SPM5, again using default parameters (smoothing of source 8 mm FWHM, 25 mm cutoff, regularization = 1).

(5) FNIRT: Non-linear normalization (Andersson et al., 2008) as recently introduced into the FSL software package (see http://fsl.fmrib.ox.ac.uk/fsl/fnirt/). The nonlinear version of the MNI152 whole-brain template and the default parameters for this template were used (masking within-brain tissue, wrap resolution of 10 mm, spline order 3, all as specified in the T1_2_MNI152_2 mm.cnf file).

(6) SUIT: Nonlinear normalization to the SUIT-template, using the default parameters from the SUIT toolbox (Diedrichsen, 2006) under SPM5 (smoothing of source 2 mm FWHM, 10 mm cutoff, regularization = 1).

Generation of probabilistic maps

After normalization of the anatomical image, the individual lobular maps were brought into the reference space by reslicing them after the same transformation using trilinear interpolation. The resliced masks were then averaged across participants. Because the original masks contained a 1 for voxels belonging to the lobule and 0 otherwise, the average lobular maps can be directly interpreted as probability maps. We also computed maximum-probability maps, which indicate for every voxel in reference space the lobular compartment with the maximal probability. The value for voxels in which this maximal probability was smaller than 0.25 was set to zero, indicating that they most likely did not belong to cerebellar gray matter. As a measure of anatomical overlap, we found for each cerebellar voxel the probability for the compartment with the highest probability, and average these values across voxels.

Results

Individual anatomy

Although individual lobules were clearly identifiable in each of the cerebella, the overall shape of the cerebellum in each subject varied markedly. This is illustrated in three individual cases in Fig. 1 (comparable coronal planes of section). For example, in some participants (e.g. Fig. 1A) lobule IX is pushed downward into the opening of the foramen magnum, whereas for the other participants (Figs. 1B, C) lobule IX is rolled inward and the neighboring lobule VIIIb forms the inferior surface of the cerebellum that extends into the mouth of the foramen magnum.

A second variable feature was the course of the ansoparamedian fissure, which defines the boundary between Crus II and VIIb. The individual cerebellum annotated by Schmahmann et al. (2000) showed an interesting asymmetry: the ansoparamedian fissure joined the horizontal fissure in the left hemisphere such that Crus II was not present laterally. This was not the case in the right hemisphere. We observed this behavior only in 3 out of 50 cerebellar hemispheres, two on the left and one on the right side (for example Fig. 1B, right). On average, however, Crus II becomes markedly smaller when moving laterally, but there is little asymmetry between the hemispheres in this respect.

Average volumes and asymmetries

To restrict the atlas to gray matter voxels, we segmented the individual scans using a probabilistic segmentation algorithm (Ashburner and Friston, 2005) and only included voxels for which the probability of gray matter was higher than the probability of white matter or of CSF. Note, however, that these "gray-matter" voxels can include small stems of white matter (often < 0.5 mm) as they are found in individual folia. Therefore, our estimated gray matter volume at a voxel size of 1 mm may be slightly higher than the true gray matter volume.

With this caveat, the average estimated gray matter volume was 118.86 cm^3 for male participants and 109.32 cm^3 for female participants ($t(18) = 1.538$, $p = 0.142$). These volumes are comparable to previous reported volumes of 112 cm^3 (Makris et al., 2005) or 108 cm^3 (for a group of female participants Keuthen et al., 2007). Dimitrova et al. (2006) also reported a similar gender difference, although this study includes all of the cerebellar white matter into the volume estimation.

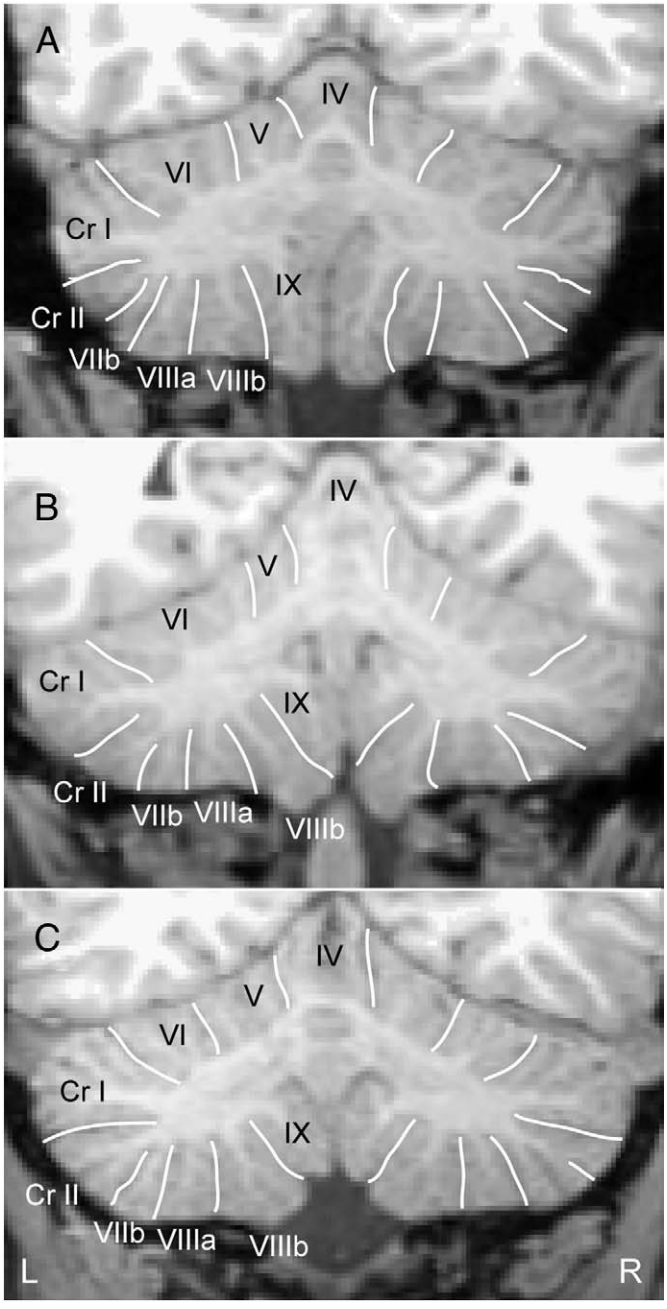

Fig. 1. Parcellation of three individual cerebella (A–C). White lines denote fissures, and Latin numerals the assignment to lobules.

Table 1
Mean volume (and standard deviation, SD) of lobules in percent of the total estimated cerebellar gray matter volume (on average 114.09 cm^3)

Lobule	Left hemisphere		Right hemisphere		Vermis		Total		Left–right asymmetry	
	Mean	SD	Mean	SD	Mean	SD	Mean	SD	$t(9)$	p
I_IV	2.83	0.67	3.11	0.61	–	–	5.94	1.24	−3.54	0.002
V	3.35	0.75	3.35	0.69	–	–	6.71	1.36	0.01	0.992
VI	7.47	0.85	6.93	0.84	1.67	0.31	16.07	1.80	5.86	0.000
Crus I	11.22	1.54	11.15	1.46	0.05	0.08	22.42	2.95	0.52	0.612
Crus II	8.58	1.46	8.11	1.30	0.38	0.12	17.07	2.46	1.57	0.134
VIIb	4.02	1.23	3.98	0.98	0.21	0.09	8.21	1.96	0.14	0.894
VIIIa	3.93	1.10	3.91	0.77	0.92	0.18	8.75	1.67	0.09	0.930
VIIIb	3.32	0.38	3.28	0.47	0.52	0.14	7.11	0.78	0.48	0.637
IX	2.85	0.76	2.97	0.71	0.64	0.13	6.46	1.48	−1.97	0.063
X	0.49	0.13	0.52	0.08	0.25	0.06	1.26	0.14	−0.62	0.544
Total	48.05	0.61	47.31	0.53	4.64	0.45	100		3.19	0.005

The vermis was not defined for the anterior lobe. The t-tests in the last column test whether the cerebellar volume was bigger on for the left or right hemisphere for that particular lobule, with positive t-values indicating greater volume on the left.

Table 1 shows a breakdown of the estimated cerebellar gray matter volume into separate compartments. The proportion of cerebellar gray matter assigned to each lobule corresponds well to previous reports (Makris et al., 2005). The data emphasizes the dominant size of the lobule VII, consisting of Crus I, CrusII, and VIIb. Lobule VII accounts for approximately half (47.70%) of the estimated gray matter volume of the human cerebellum, compared to approximately a quarter (24.37%) in the Capuchin monkey (Balsters et al., 2008). There was no gender difference in terms of the relative lobular volumes (gender×lobule interaction $F(9,18)=0.369$).

Interestingly, we observed a significant pattern of hemispheric asymmetry in our sample. Overall, the left hemisphere of the cerebellum was larger than the right hemisphere, $t(19)=3.18$, $p=0.005$. While anterior lobules III and IV show bigger volume for the right than for the left hemisphere, the opposite pattern was observed in lobule VI. This asymmetry pattern has been described earlier and is possibly related to handedness (Snyder et al., 1995). While the left–right difference did not interact significantly with gender ($F(1,18)=2.964$, $p=0.10$), numerically the hemispheric asymmetry was slightly more pronounced in male than in female participants.

Overlap after normalization

We used a number of different normalization methods to bring the individual cerebellar anatomy into a common reference space. In doing so, we could compare the quality of the overlap of cerebellar structures after normalization using these methods. Furthermore, we could also assess possible spatial biases that arise from the different normalization methods for our sample.

The average overlap of cerebellar lobules across individuals (see Methods) was 49% for affine registration without skull stripping, 57% for the standard non-linear normalization using SPM5, 61% for affine registration (FLIRT) after skull stripping, 67% after segmentation and simultaneous normalization in SPM5, 68% for nonlinear alignment in FSL (FNIRT), and 75% after normalization to the SUIT template. Thus, a marked improvement in cerebellar normalization can be obtained if only within-cerebellar tissue is considered, and if a cerebellum-specific template is employed.

The spatial distribution of the maximal probability illuminates the strength and weaknesses of intensity-based normalization methods. For normalization using SUIT (Fig. 2A), there were areas within each lobular volume in which the probability values reached 1, indicating that all subjects overlapped with the same lobule. This is naturally more pronounced for the larger lobules (Crus I and II) than for the smaller lobules one on the inferior surface of the cerebellum (VIIIa and VIIIb). However, even these lobules reached perfect overlap in the centre of the averaged representation. This demonstrates the efficacy of intensity-based 3D normalization methods for the human cerebellum. The average overlap after affine registration using FLIRT (Fig. 2B) was consistently poorer than SUIT normalization, but revealed a similar general pattern.

The resulting overlap also clearly shows which cerebellar features can be reliably normalized using intensity-based normalization, and where the technique is limited. While the primary fissures of individual brains superimpose very accurately in the vermis, the superposition becomes progressively poorer when moving laterally (Fig. 3). This is because the primary fissure is well defined by intensity information on mid-saggital slices, but cannot easily be seen on more lateral slices, where one can only identify it by following the primary fissure from the vermis outward. Table 2 summarizes the average overlap for each of all

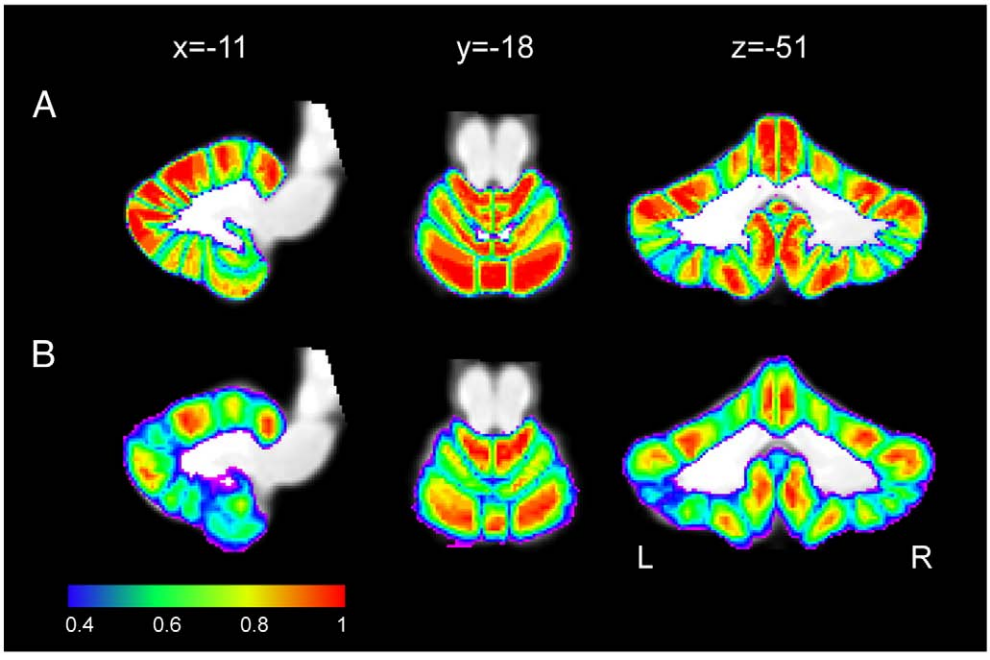

Fig. 2. Saggital, horizontal and coronal slices through combined probabilistic maps of each lobule. The colors indicate the size of the maximal probability after (A) non-linear normalization to the SUIT template and (B) affine registration (FLIRT) to the MNI152-whole brain template. A high probability reached in each compartment indicates good overlap.

Please cite this article as: Diedrichsen, J., et al., A probabilistic MR atlas of the human cerebellum, NeuroImage (2009), doi:10.1016/j.neuroimage.2009.01.045

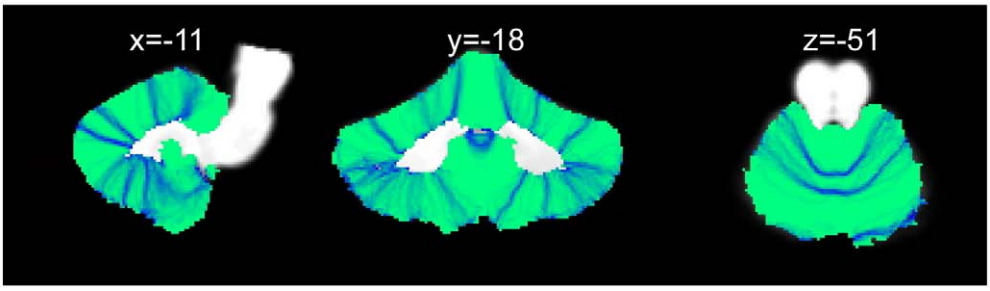

Fig. 3. Overlap of fissures after SUIT normalization. Light green shading indicates no fissure in this voxel, a dark blue indicates that all 20 fissures overlapped in that particular voxel. Clearly visible on the horizontal slice ($z=-51$) is the fact that the primary fissure overlaps well in the vermis, but overlap becomes poorer when moving laterally. On the saggital ($x=-11$) slice one can see the good overlap for the horizontal fissure, but poorer overlap for other fissures. (For interpretation of the references to colour in this figure legend, the reader is referred to the web version of this article.)

identified fissures. After SUIT normalization, the posterior-lateral and horizontal fissures are superimposed more tightly then the fissures in the inferior cerebellum, partly because these latter fissures are not as well defined by intensity information. Similar differences between fissures are also found using affine normalization (FLIRT, see Table 2), indicating that partly these differences are also caused by differences in the anatomical variability of fissures.

To assess the correspondence between different normalization methods, we compared the probability-maps for the five main normalization methods we applied here. Fig. 4 shows the outline of the averaged cerebellum on a coronal slice after normalization with different methods. As reported previously (Diedrichsen, 2006), non-linear normalization as implemented as a standard in SPM2/5 leads on average to a cerebellar representation that is elongated in the *z*-direction compared to other methods. In contrast, other normalization methods (FLIRT, FNIRT, SPM segmentation, SUIT) are in good spatial correspondence. The best agreement for any pair of these three methods existed between SUIT and FNIRT, with only 1.75% of the voxels in the cerebellar volume assigned to different compartments. This indicates that the latter four normalization methods, three of which are using a different reference template, are reasonably unbiased in relation to each other.

Probabilistic atlases

The resulting probabilistic atlas(es) consist of a set of 28 probabilistic maps indicating the likelihood that a certain voxel in reference space belongs to each lobular compartment. As a summary, we also computed a maximum-probability map, which indicates the compartment that has the highest probability. We calculated these maps directly from the normalized, unsmoothed probability maps.

Strictly speaking, the use of a probabilistic atlas is only valid when the functional or anatomical data is analyzed using the same normalization method that had been employed for the generation of the atlas. Simply relying on the fact that the data is in "MNI Space" is insufficient. As shown, the non-linear normalization as implemented in SPM2/5 leads to a mean cerebellum that is systematically elongated in the *z*-direction by approximately 1 cm. We publish the atlas for this normalization method, because we think it will prove useful for the interpretation of existing imaging studies. For new cerebellar studies, however, we would discourage the use of this normalization method, because of its spatial bias and its inferior performance in terms of overlap. The other normalization methods led to unbiased results and only differ in terms of the certainty of the lobular assignment. FNIRT and segmentation and normalization in SPM5 led to similar results and we therefore provide only one version of the atlas for these two method. A separate atlas is published for the SUIT method, which resulted in the best overlap after normalization.

To view and to employ probabilistic atlases to anatomical and functional imaging data, a number of different tools have been developed over recent years. These include the atlas widget in FSLView (Smith et al., 2004), maximum-probability-maps in MRICroN (Rorden, 2007), and the Anatomy toolbox in SPM (Eickhoff et al., 2005). To maximize the utility of the atlas, we have prepared versions in formats that are compatible with these three utilities (see http://www.bangor.ac.uk/~pss412/imaging/propatlas.htm). Fig. 5 shows an example of how the atlas can be used with MRICroN to assign an anatomical label to a functional activation in a group analysis.

Table 2
Average overlap of reconstructed fissures after affine (FLIRT) and nonlinear (SUIT) normalization

Fissure	Overlap after FLIRT normalization	Overlap after SUIT normalization
Intraculminate	12.6%	19.4%
Primary	10.4%	17.5%
Superior posterior	12.1%	22.6%
Horizontal	11.1%	23.8%
Ansoparamedian	11.9%	18.02%
Prebiventer	11.9%	18.05%
Intrabiventer	10.9%	18.8%
Secondary	12.5%	19.9%
Postero-lateral	14.0%	25.2%

The overlap is calculated as the percentage of participants, for whom the surface of a given fissure ran through a given 1×1×1 mm voxel, averaged over all the voxels, which contained the fissure of at least 1 participant.

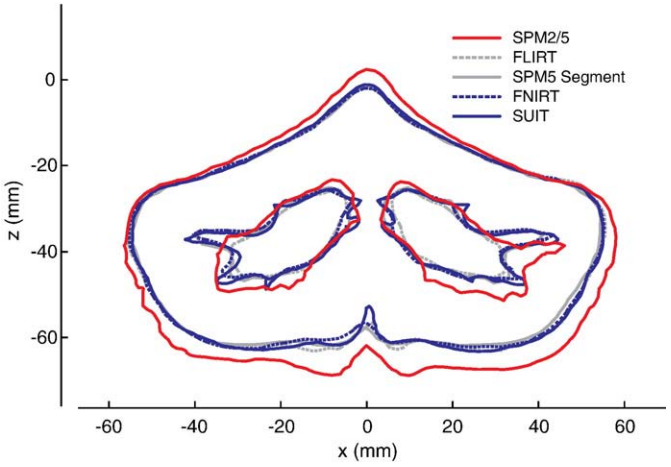

Fig. 4. Correspondence between different normalization methods. Shown is outline of the mean cerebellum in atlas space, thresholded at a 0.5 probability for being in any lobular compartment for a coronal slice ($y=-62$ mm). While linear (FLIRT) and non-linear (FNIRT) normalization in FSL, SUIT, and normalization and segmentation in SPM5 (SPM5 Segment) lead to mutually unbiased results, the standard nonlinear normalization (SPM2/5) results in an elongated cerebellum.

Please cite this article as: Diedrichsen, J., et al., A probabilistic MR atlas of the human cerebellum, NeuroImage (2009), doi:10.1016/j.neuroimage.2009.01.045

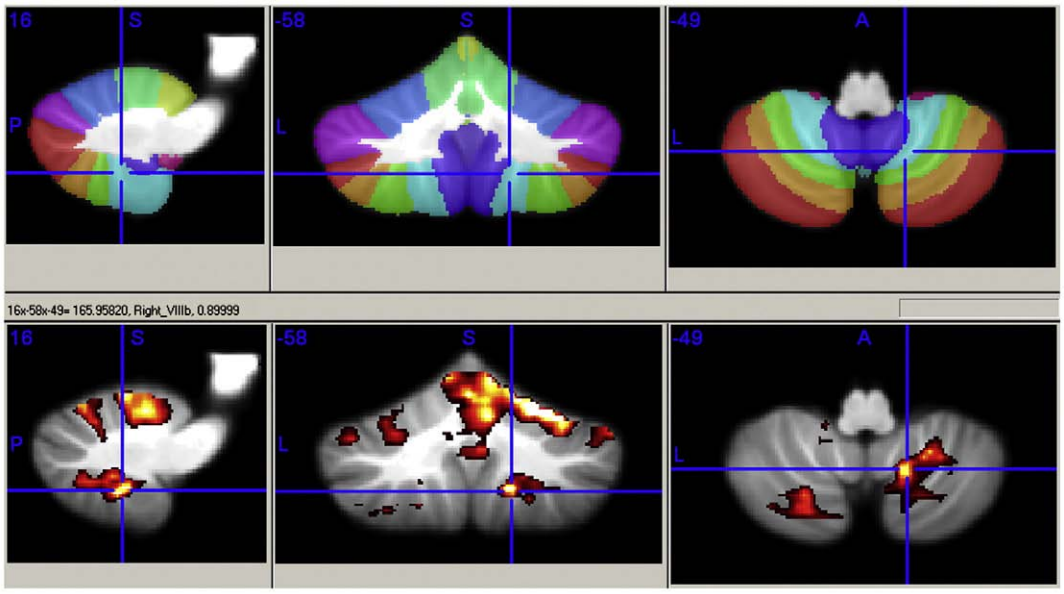

Fig. 5. Assignment of lobular labels to foci of activations from a group study using the probabilistic atlas for MRICroN (Rorden, 2007) and the cerebellum-only atlas template (Diedrichsen, 2006). Upper window shows a color-coded map of the lobule with the maximum probability. The bar below the window denotes the position in SUIT space (16, −58, −49), the name of the lobule (VIIIb, right hemisphere), and the size of that probability (89%). The lower window shows group activation map of right arm movement. (For interpretation of the references to colour in this figure legend, the reader is referred to the web version of this article.)

Example of the use of ROIs defined by the maximal-probability-map

To further demonstrate the potential utility of probabilistic atlases, we employed here ROIs defined by the maximum-probability map to functional imaging data. Two groups of participants made either left or right arm reaching movements using a MRI-compatible robotic manipulandum (Diedrichsen et al., 2007). Based on the maximum probability maps of the atlas in SUIT space, each voxel was assigned one of 28 cerebellar compartments, and the average percent signal change for each of these ROIs was extracted for each participant (Fig. 6). Activity was observed in the anterior lobe, strictly ipsilateral to the arm movement. Lobule VI showed more bilateral activation, possibly indicating that lobule VI, although it receives direct input from primary motor cortex, may also get input from premotor and parietal regions, which usually show bilateral activation during unimanual movements. Congruent with this notion lobule VI has been shown to have role in movement preparation (Hulsmann et al., 2003). The hemispheres of Crus I and II were hardly activated, while strong activity was observed in the vermis of lobule VII, possibly related to an involvement in eye movement (Baizer et al., 1999). Finally, in the inferior cerebellum, activity was observed in the secondary motor representation, including lobules VIIb, VIIIa (Kelly and Strick, 2003) and possibly also VIIIb. Here the activity was biased towards the ipsilateral side as well, however, this was less pronounced than in the primary motor representation of the anterior lobe. In sum, ROIs defined by maximum probability maps provide a detailed and efficient way to summarize functional data.

Discussion

The cerebellar atlas developed here relies on macro-anatomical landmarks to distinguish different lobules in the human cerebellum, following the current consensus in nomenclature (Schmahmann et al., 2000). This approach contrasts with recent probabilistic atlases of the human neocortex that are based on cytoarchitectonic information (Amunts and Zilles, 2001; Toga et al., 2006). While there are some chemical markers that indicate a compartmentalization of the cerebellum (Herrup and Kuemerle, 1997), these markers mostly divide the cerebellum in a set of parasaggital zones. There are no known markers applicable in humans that would distinguish areas of different functional connectivity. A purely macro-anatomical approach is also more feasible in the cerebellum than in the neocortex, given that the overall cerebellar structure, the number and form of major fissures, is highly consistent across individuals. The extent to which lobular boundaries reflect borders in input–output relations has been informed by a few studies (Kelly and Strick, 2003) but is an important question for further research.

While the MRI atlas of the human cerebellum (Schmahmann et al., 2000) was a major step forward, only a probabilistic atlas based on multiple individuals can serve as a valid reference for lobular assignments to group-normalized data. It also provides a measure of the certainty with which assignments can be made. The importance of a valid atlas becomes especially clear when taking into account the differences in normalization methods that are currently in use. While four of the normalization methods (FLIRT, FNIRT, SPM5 with concurrent segmentation and SUIT) had a high degree of agreement, the non-linear normalization without segmentation (standard normalization in SPM2 and SPM5) led to a significant spatial bias. This fact needs to be taken into consideration both when choosing an anatomical reference for a particular study, but also when performing meta-analyses to integrate results across different studies that utilize different normalization methods.

We hope that the new atlas(es) will be a useful tool for further research into the structure and function of the human cerebellum. Primarily, the atlas can serve as an unbiased reference to assign lobular labels to the foci of activation in group analyses of MRI studies. In an ideal world, one would of course prefer if all researchers would determine lobular boundaries on each of the individuals studied (e.g. Desmond et al., 1997), and make lobular assignment based on this information. However, such procedure is work intensive and requires a considerable level of anatomical expertise and training, and is consequently not very often employed for group MRI studies. Instead researchers often make lobular assignments based on anatomical information from a single individual, or they rely on an atlas reference template that does not have enough anatomical detail to determine lobular boundaries reliably. In these cases the probabilistic atlas will reduce the risk of localization errors by providing researchers with a valid and unbiased anatomical reference. In short, we hope the atlas will widen the access to detailed cerebellar anatomy to non-expert investigators.

Please cite this article as: Diedrichsen, J., et al., A probabilistic MR atlas of the human cerebellum, NeuroImage (2009), doi:10.1016/j.neuroimage.2009.01.045

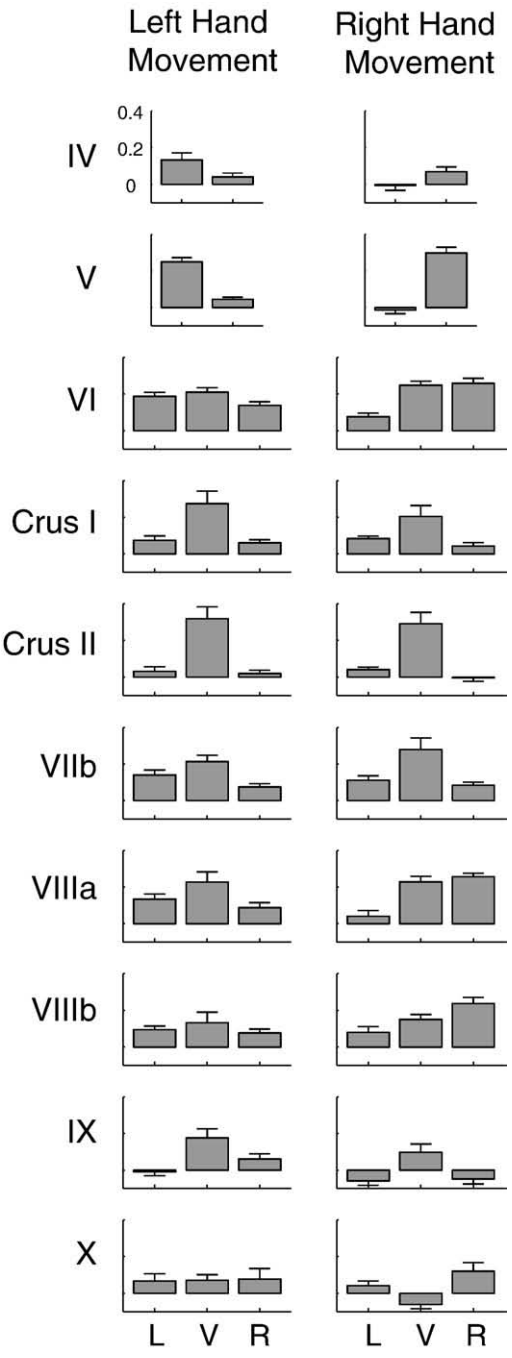

Fig. 6. Functional analysis using regions-of-interest defined by maximal probability maps. The bars indicate average percent signal change during left or right arm pointing movements for the left hemisphere (L), vermis (V) and right hemisphere (R) of each cerebellar lobule.

Secondly, probabilistic atlases also quantify the degree of certainty with which anatomical assignment can be made. This allows us to critically evaluate and integrate empirical evidence. At the same time, the certainty measures provide a comparison of different commonly-used normalization methods. Here we found that cerebellum-only normalization as implemented in SUIT (Diedrichsen, 2006) outperformed all whole-brain normalization methods, even when compared to a normalization method that uses a comparable resolution of non-linear deformation (1 cm), and a nonlinear template with good anatomical details of the cerebellar lobules (FNIRT). This suggests that the prior automated separation of cerebellar and cerebral gray matter maybe beneficial for the quality of normalization. However, it is possible that other differences between the methods, such as the exact choice of regularization parameters, may influence these results. While investigating all factors that determine the quality of cerebellar overlap after normalization is beyond the scope of this paper, we suggest that this the data set can serve as an important benchmark test for future normalization and parcellation algorithms.

Third, the atlas can be used to define regions-of-interest based on maximum-probability maps (Eickhoff et al., 2006). As shown here for the example of functional activations elicited by arm-movements, these ROIs allow for a valid and fast way of extracting data for a group of participants from predefined areas. This can be done not only for functional data, but also for structural data such as that used for voxel-based morphometry (VBM, Ashburner and Friston, 2000) and for lesion analysis (Rorden and Brett, 2001). This technique has the distinct advantage to allow testing of a-priori defined hypotheses without the need to correct for multiple tests.

Finally, while our results show the strength of automatic intensity-based normalization methods, they also point to limitations: for some fissures (e.g. the lateral aspects of the primary fissures), these methods fail achieve a good registration between individuals. Therefore, for some detailed studies of cerebellar anatomy or pathology it may still be necessary to employ hand-parcellation or semi-automatic algorithms that assign voxels to lobules based on detailed information about the course of the fissures (Makris et al., 2003; Makris et al., 2005). The probabilistic atlas can serve as a prior probability map to improve the ease and speed of such methods. With the atlas we also publish a Matlab function that allows the deformation of the maximum probability maps into the individual anatomical space. These maps then can serve as a starting point for manual segmentation, saving considerable effort.

We hope that the class of probabilistic atlases of the human cerebellum will be a generally useful tool and help to improve our knowledge about the functional heterogeneity of this fascinating part of the brain. Various versions of the atlas based on different normalization methods and image analysis packages are available at http://www.bangor.ac.uk/~pss412/imaging/propatlas.htm.

Acknowledgments

The work was supported by Grants from the National Science Foundation (BSC 0726685, to JD), and the Biological Sciences Research Council (to NR). JHB was supported by RHUL-SGUL joint scholarship awarded to NR; EC supported by Welcome Trust Vacation Scholarship to NR and EC. We thank John Schlerf for helpful comments.

References

Amunts, K., Zilles, K., 2001. Advances in cytoarchitectonic mapping of the human cerebral cortex. Neuroimaging Clin. N. Am. 11, 151–169 vii.
Andersson, J.L., Smith, S.M., Jenkinson, M., 2008. FNIRT— FMRIB's non-linear image registration tool. Poster presented at the annual meeting of the Organization Hum. Brain Mapp., Melbourne, Australia.
Ashburner, J., Friston, K.J., 1999. Nonlinear spatial normalization using basis functions. Hum. Brain Mapp. 7, 254–266.
Ashburner, J., Friston, K.J., 2000. Voxel-based morphometry—the methods. Neuroimage 11, 805–821.
Ashburner, J., Friston, K.J., 2005. Unified segmentation. NeuroImage 26, 839–851.
Baizer, J.S., Kralj-Hans, I., Glickstein, M., 1999. Cerebellar lesions and prism adaptation in macaque monkeys. J. Neurophysiol. 81, 1960–1965.
Balsters, J.H., Cussans, E., Diedrichsen, J., Philips, K., Preuss, T.M., Rilling, J.K., Ramnani, N., 2008. Evolution of the cerebellar cortex: selective expansion of prefrontal projecting lobules. Poster presented at the annual meeting of the Organization Hum. Brain Mapp., Melbourne, Australia.
Desmond, J.E., Gabrieli, J.D., Wagner, A.D., Ginier, B.L., Glover, G.H., 1997. Lobular patterns of cerebellar activation in verbal working-memory and finger-tapping tasks as revealed by functional MRI. J. Neurosci. 17, 9675–9685.
Diedrichsen, J., 2006. A spatially unbiased atlas template of the human cerebellum. NeuroImage 33, 127–138.
Diedrichsen, J., Criscimagna-Hemminger, S.E., Shadmehr, R., 2007. Dissociating timing and coordination as functions of the cerebellum. J. Neurosci. 27, 6291–6301.
Dimitrova, A., Zeljko, D., Schwarze, F., Maschke, M., Gerwig, M., Frings, M., Beck, A., Aurich, V., Forsting, M., Timmann, D., 2006. Probabilistic 3D MRI atlas of the human cerebellar dentate/interposed nuclei. NeuroImage 30, 12–25.

Eickhoff, S.B., Stephan, K.E., Mohlberg, H., Grefkes, C., Fink, G.R., Amunts, K., Zilles, K., 2005. A new SPM toolbox for combining probabilistic cytoarchitectonic maps and functional imaging data. NeuroImage 25, 1325–1335.
Eickhoff, S.B., Heim, S., Zilles, K., Amunts, K., 2006. Testing anatomically specified hypotheses in functional imaging using cytoarchitectonic maps. NeuroImage 32, 570–582.
Eickhoff, S.B., Paus, T., Caspers, S., Grosbras, M.H., Evans, A.C., Zilles, K., Amunts, K., 2007. Assignment of functional activations to probabilistic cytoarchitectonic areas revisited. NeuroImage 36, 511–521.
Evans, A.C., Collins, D.L., Mills, S.R., Brown, E.D., Kelly, R.L., Peters, T.M., 1993. 3D statistical neuroanatomical models from 305 MRI volumes. Proc. IEEE-Nuclear Sci. Symp. Med. Imagine Conf. 1813–1817.
Friston, K., Holmes, A.P., Ashburner, J., 1999. Statistical Parameter Mapping (SPM).
Herrup, K., Kuemerle, B., 1997. The compartmentalization of the cerebellum. Annu. Rev. Neurosci. 20, 61–90.
Hulsmann, E., Erb, M., Grodd, W., 2003. From will to action: sequential cerebellar contributions to voluntary movement. NeuroImage 20, 1485–1492.
Jenkinson, M., Bannister, P., Brady, M., Smith, S., 2002. Improved optimization for the robust and accurate linear registration and motion correction of brain images. NeuroImage 17, 825–841.
Kelly, R.M., Strick, P.L., 2003. Cerebellar loops with motor cortex and prefrontal cortex of a nonhuman primate. J. Neurosci. 23, 8432–8444.
Keuthen, N.J., Makris, N., Schlerf, J.E., Martis, B., Savage, C.R., McMullin, K., Seidman, L.J., Schmahmann, J.D., Kennedy, D.N., Hodge, S.M., Rauch, S.L., 2007. Evidence for reduced cerebellar volumes in trichotillomania. Biol. Psychiatry 61, 374–381.
Makris, N., Hodge, S.M., Haselgrove, C., Kennedy, D.N., Dale, A., Fischl, B., Rosen, B.R., Harris, G., Caviness Jr., V.S., Schmahmann, J.D., 2003. Human cerebellum: surface-assisted cortical parcellation and volumetry with magnetic resonance imaging. J. Cogn. Neurosci. 15, 584–599.
Makris, N., Schlerf, J.E., Hodge, S.M., Haselgrove, C., Albaugh, M.D., Seidman, L.J., Rauch, S.L., Harris, G., Biederman, J., Caviness Jr., V.S., Kennedy, D.N., Schmahmann, J.D., 2005. MRI-based surface-assisted parcellation of human cerebellar cortex: an anatomically specified method with estimate of reliability. NeuroImage 25, 1146–1160.
Middleton, F.A., Strick, P.L., 1997. Cerebellar output channels. In: Schahmann, J.D. (Ed.), The Cerebellum and Cognition. Academic Press, San Diego, CA, pp. 31–60.
Ramnani, N., 2006. The primate cortico-cerebellar system: anatomy and function. Nat. Rev. Neurosci. 7, 511–522.
Rorden, C., 2007. MRICroN.
Rorden, C., Brett, M., 2001. Stereotaxic display of brain lesions. Behav. Neurol. 12, 191–200.
Schmahmann, J.D., Doyon, J., Toga, A., Petrides, M., Evans, A., 2000. MRI Atlas of the Human Cerebellum. Academic Press, San Diego.
Smith, S.M., Jenkinson, M., Woolrich, M.W., Beckmann, C.F., Behrens, T.E., Johansen-Berg, H., Bannister, P.R., De Luca, M., Drobnjak, I., Flitney, D.E., Niazy, R.K., Saunders, J., Vickers, J., Zhang, Y., De Stefano, N., Brady, J.M., Matthews, P.M., 2004. Advances in functional and structural MR image analysis and implementation as FSL. NeuroImage 23 (Suppl. 1), S208–S219.
Snyder, P.J., Bilder, R.M., Wu, H., Bogerts, B., Lieberman, J.A., 1995. Cerebellar volume asymmetries are related to handedness: a quantitative MRI study. Neuropsychologia 33, 407–419.
Toga, A.W., Thompson, P.M., Mori, S., Amunts, K., Zilles, K., 2006. Towards multimodal atlases of the human brain. Nat. Rev. Neurosci. 7, 952–966.

Please cite this article as: Diedrichsen, J., et al., A probabilistic MR atlas of the human cerebellum, NeuroImage (2009), doi:10.1016/j.neuroimage.2009.01.045